Nanoscale creep modelling on calcium-silicate-hydrates using molecular dynamics simulation

Sela Hoeun[1], Frédéric Grondin[1], Ahmed Loukili[1]

[1] *Nantes Université, Ecole Centrale Nantes, CNRS, GeM, UMR 6183, F-44000 Nantes, France*

RESUME Sous une charge externe constante, les matériaux solides subissent une déformation élastique immédiate, suivie de déformations dépendantes du temps, un phénomène appelé fluage. Dans les structures en béton, les hydrates de silicate de calcium (C-S-H), représentant au moins 50 % du volume de la pâte de ciment hydratée durcie, contribuent de manière significative à leur résistance. Le fluage du béton est aujourd'hui assez bien prédit par la modélisation multi-échelles avec des propriétés matériaux qui sont dépendantes du modèle choisi et ne sont donc pas intrinsèques au sens physique. Pour modéliser des nouveaux bétons, avec des mélanges bas carbone par exemple, il est nécessaire de mettre à jour les données matériaux. Dans cette étude, il est proposé de définir des propriétés visco-élastiques intrinsèques du C-S-H afin de proposer une modélisation thermodynamique du fluage des matériaux cimentaires. Un modèle de dynamique moléculaire a été choisi pour réaliser des tests de traction sous contrainte constante à l'échelle nanométrique sur un composite de phases de C-S-H. Les variations d'espacement et d'orientation des composites ont été analysées dans différents scénarii. Des courbes de déformation en fonction du temps à l'échelle nanométrique ont été déterminées.

Mots-clefs Dynamique Moléculaire, Silicate de calcium hydraté, fluage

I. INTRODUCTION

Cementitious materials, which are widely used, have a heterogeneous composition on various scales. The behaviour of concrete, particularly in terms of cracking, is still not fully controlled due to its complex structure. Concrete is a composite material made up of a cement matrix (the binding phase) and aggregates (the inclusion phase). As a result, the mechanical properties of concrete are greatly affected by the cement matrix (Keinde et al., 2014; Lau et al., 2018). Furthermore, the cement matrix is a porous material with a multiscale structure, exhibiting different physical properties at various length scales (Ioannidou, 2020). For example, calcium-silicate-hydrates (C-S-H) are the main component of hardened hydrated cement paste (Lau et al., 2018). The concrete industry searches for developing low-carbon concrete and would like to perform materials having the best durability. The composition of low-carbon concrete should be well defined by knowing the best relationships between properties of each component and the macroscopic behaviour to reach. The civil engineer is mainly interested in the fracture behaviour under static and dynamic loadings. Also, in the case of large structure, a high interest concerns the creep behaviour when concrete is submitted to a constant loading. The prediction of creep of low-carbon concrete needs to well known the influence of each component. Most theories suppose that the creep of concrete is mainly

due to the water movement into C-S-H, which creates a displacement of C-S-H layers. Is it really true?

According to the fact that the adsorbed water on C-S-H exhibits a high adhesive contact, which needs very high pressure to separate them, recent works have considered that creep could be mainly due to C-S-H blocks displacement, but not water movement between C-S-H layers (Guo et al., 2019; Rhardane et al., 2022). The observation of these assumptions has never been observed due to the difficulty to follow the phenomena into the microstructure during the test. Numerical methods based on multiscale approaches have been developed to give an answer but it is too dependent on the visco-elastic model type. Indeed, in multiscale modelling, it is first crucial to determine the mechanical properties of the hydrated cement phases. One method for obtaining these properties is through the use of nano-indentation testing (Bekrine et al., 2025; Fu et al., 2018b). An alternative widely used method is molecular dynamics simulations which has already shown the relevance for the determination of fracture properties (Hoeun et al., 2023).

In this article, we did the nanoscale creep modelling on C-S-H using molecular dynamics simulation. The results presented might serve to bring an idea on the role of adsorbed water on the C-S-H and to define input parameters for higher-scale modelling, such as the microscopic scale of cementitious materials. Two C-S-H phases, when combined, form a "composite," and different spacing configurations and orientations of these phases are investigated. Creep tests were performed at a constant load of 30%, as recommended in experimental creep tests, of the peak stress obtained in the tensile tests. The deformation versus time curves were obtained and the compliance properties were determined. Discussion is proposed on the influence of the adsorbed water on creep of C-S-H.

II. MATERIALS AND MODELS

The C-S-H phase forms when C_3S hydrates. It shares structural similarities with crystalline phases like jennite and 11 Å tobermorite (Hewlett, 1998). The C-S-H phase can be classified into calcium-rich or silicon-rich forms based on the Ca/Si ratio. It is further divided into C-S-H (I) with a Ca/Si ratio ranging from 0.6 to 1.5, and C-S-H (II) with a Ca/Si ratio between 1.5 and 2.0. 11 Å tobermorite unit cell has a chemical formula $Ca_4Si_6O_{14}(OH)_4{\cdot}2H_2O$, cell lengths (a, b, c) = (6.69 Å, 7.39 Å, 22.779 Å) and cell angles (α, β, γ) = (90°, 90°, 123.49°) as shown in Fig. 1 (Hamid, 1981). Its crystal structure is monoclinic, belonging to the $P2_1$ space group. Using the annealing process, (Fu et al., 2018a) developed C-S-H (I) initially from 11 Å tobermorite. We applied the same method and obtained the C-S-H (I) with a Ca/Si ratio of 0.67. Open Visualization Tool (OVITO) was utilized for visualization (Stukowski, 2009). Molecular dynamics is a computational simulation method used to study the physical movement of atoms and molecules. It calculates the trajectories of atoms and molecules by numerically solving Newton's equations of motion for a system of interacting particles. The potential energy and interatomic forces are determined using interatomic potentials or mechanical force fields of the molecules (Plimpton, 1995). The Large-scale Atomic/Molecular Massively Parallel Simulator (LAMMPS) was used to carry out the creep test simulations. In this simulation, each of the N atoms or molecules is treated as a point mass, and Newton's equations of motion are integrated to compute their movement (Plimpton, 1995).

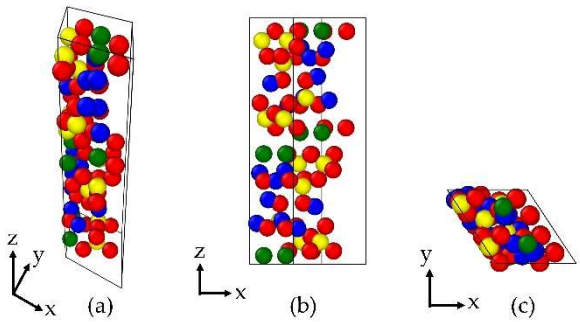

FIGURE 1. **Unit cell of 11 Å tobermorite: (a) perspective view, (b) xz-plane and (c) xy-plane. Green balls = Ca atoms, yellow balls = Si atoms, red balls = O atoms, blue balls = H atoms.**

The ReaxFF force field (van Duin et al., 2001) can be applied to model the main phases of hydrated cement. The ReaxFF parameters used in this study are detailed in (Liu et al., 2012). The total system energy can be expressed as follows (van Duin et al., 2001):

$$E_{system} = E_{bond} + E_{over} + E_{under} + E_{val} + E_{pen} + E_{tors} + E_{conj} + E_{vdWaals} + E_{Coulomb} \quad (1)$$

where E_{bond}, E_{over} and E_{under} represent respectively the bond energy, the energy penalty for over- and under-coordination of atoms. E_{val}, E_{pen}, E_{tors}, E_{conj}, $E_{vdWaals}$ and $E_{Coulomb}$ represent respectively the valence angle, penalty, torsion, conjugation, van der Waals and Coulomb energy.

One of difficulty to model the creep behaviour of cementitious materials is the choice of the creep model. According to the model, the visco-elastic properties are not exactly the same and it could affects the results. In this work, three models have been tested in order to see if the dynamic molecular approach is intrinsic. For viscoelastic models, Maxwell model is represented by an elastic spring and a viscous damper arranged in series, whereas Kelvin-Voigt model is represented by an elastic spring and a viscous damper arranged in parallel. On the other hand, Burgers model is composed of the Maxwell and Kelvin-Voigt models arranged in series as shown in Fig. 2.

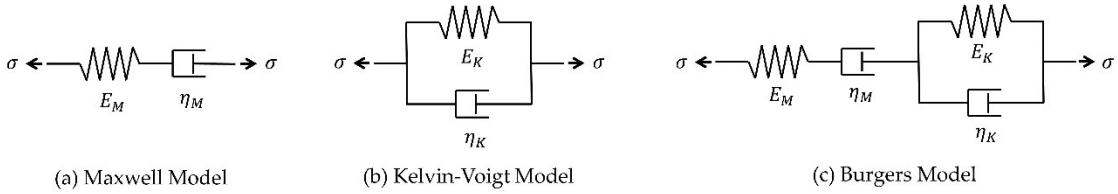

FIGURE 2. **Viscoelastic models: (a) Maxwell model, (b) Kelvin-Voigt model and (c) Burgers model**

The strain variation over time of Burgers model can be expressed as follows (Esposito et al., 2021):

$$\varepsilon(t) = \frac{\sigma_0}{E_M} + \frac{\sigma_0}{E_K}\left(1 - e^{-\frac{tE_K}{\eta_K}}\right) + \frac{\sigma_0}{\eta_M}t \quad (2)$$

where $\boldsymbol{\sigma_0}$ represents the amplitude of the imposed stress at the time $\boldsymbol{t_0}$, $\boldsymbol{E_M}$ and $\boldsymbol{\eta_M}$ the Young's modulus and the viscosity of Maxwell section, $\boldsymbol{E_K}$ and $\boldsymbol{\eta_K}$ the Young's modulus and the viscosity of Kelvin-Voigt section.

III. METHOD

The mechanical and fracture properties of the C-S-H/portlandite composite were investigated by (Liang, 2020). The unit cells of C-S-H and portlandite were extended in the x-, y-, and z-directions. Supercells were then relaxed using the NPT ensemble at a pressure of 0 Pa and a temperature of 300 K along the x-, y-, and z-directions. After relaxation, the supercells were positioned together with an interface gap of approximately 3 Å. This composite was subsequently relaxed once more using the NPT ensemble. Similarly, C-S-H (I) unit cell were replicated by 7 × 8 × 2 in the x-, y-, and z-directions, respectively. The C-S-H (I) supercell was then transformed from monoclinic structures into orthogonal supercells to obtain independent results for each direction. MD simulations were performed using the ReaxFF force field with real units in three dimensions (3D). A periodic boundary condition (PPP) was applied to eliminate boundary effects. These supercells were relaxed at a temperature of 300 K and a pressure of 0 atm using the NPT ensemble in the x-, y-, and z-directions for 50 ps. (Bonnaud et al., 2016) investigated three different orientations of C-S-H particle pairs to examine the interaction grand potential at the molecular level. These orientations were selected to account for the anisotropy effect in the geometry and crystallography of C-S-H particles. Additionally, the interaction forces between particles may be influenced by the orientations. In this study, three different orientations were selected, similar to those in (Bonnaud et al., 2016). Firstly, C-S-H (I) supercell was placed beside C-S-H (I) supercell in the y-direction. Secondly, C-S-H (I) supercell was counterclockwise 90° rotated around the x-axis and was placed beside C-S-H (I) supercell in the y-direction. Lastly, C-S-H (I) supercell was positioned on top of C-S-H (I) supercell in the z-direction. In the second case, the bottom of C-S-H (I) supercell was placed beside C-S-H (I) supercell. These orientations were illustrated in Fig. 3.

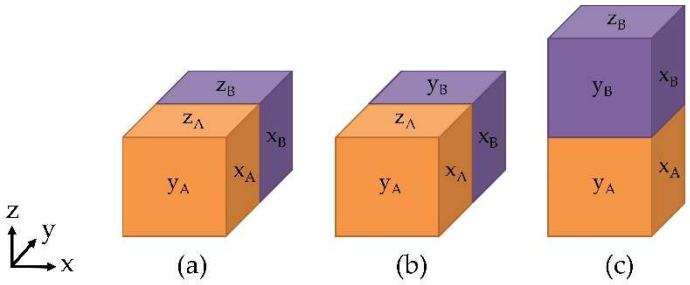

FIGURE 3. Orientations of composite phase: (a) supercell-B on the side of supercell-A in y-direction, (b) counterclockwise 90° rotated supercell-B around x-axis on the side of supercell-A in y-direction, and (c) supercell-B on top of supercell-A in z-direction.

Additionally, 1 Å interfacial vacuum layer and 3.1 Å interfacial water layer were introduced at the interface between the relaxed C-S-H (I) composite. The 1 Å interfacial vacuum layer was intended to represent an interface without porosity, while the 3.1 Å interfacial water layer was used to simulate interfaces with porosity filled with adsorbed water. The C-S-H (I) composite was then

relaxed again using the NPT ensemble for an additional 50 ps. These simulations were performed with a timestep of 0.25 fs.

Although in many ways similar to (Liang, 2020), the creep tests were investigated in this study. Creep tests were performed at a constant load of 30% of the peak stress obtained from the tensile tests. The load was applied along the y- or z-directions, coupled with relaxation in the lateral directions. The deformation versus time curves were then obtained. By fitting the curves with Burgers model using Eq. (2), the Young's modulus and the viscosity parameters of Maxwell and Kelvin-Voigt sections could be derived. To conduct simulations on C-S-H (I) composite, 48 cores of compute CPU were employed. The simulations were done by a GLiCID computing center consisted of 48 compute nodes (each with 2x AMD EPYC Genoa 9474F 48-Core, and 384GB or 768GB DDR5 memory @4800MT/s).

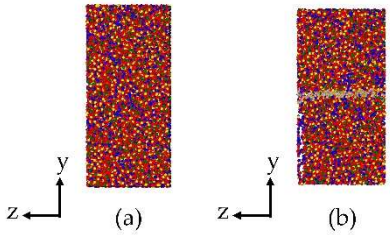

FIGURE 4. **C-S-H (I) composite phase with the interfacial (a) 1 Å vacuum layer and (b) 3.1 Å water layer.**

IV. RESULTS AND DISCUSSION

TABLE 1. **Tensile strengths.**

1 Å vacuum			3.1 Å water		
y-direction	counterclockwise rotated in y-direction	z-direction	y-direction	counterclockwise rotated in y-direction	z-direction
4.53 GPa	4.47 GPa	4.67 GPa	1.13 GPa	1.43 GPa	1.07 GPa

First of all, the tensile strength of each composites has been calculated and presented in Table 1. Fig. 5 and Fig. 6 show the strain versus time curves of C-S-H (I)/vacuum (1 Å)/C-S-H (I) composite and C-S-H (I)/water (3.1 Å)/C-S-H (I) composite in various orientations. Various viscoelastic models were used to fit the curves, i.e., Maxwell, Kelvin-Voigt and Burgers models. As could be observed, the coefficients of determination for Burgers model were the highest compared to the other models, indicating that the Burgers model could represent well the creep behaviour of the C-S-H (I) composite. Orientations and interfacial vacuum/water layers could also affect the strain versus time curves. The orientation, where the C-S-H (I) supercell was counterclockwise rotated around the x-axis and was placed beside the C-S-H (I) supercell in the y-direction, exhibited the highest strain compared to the other orientations. This means that this orientation might have lower interaction at the interface in response to the creep test. However, the other two orientations produced similar curves.

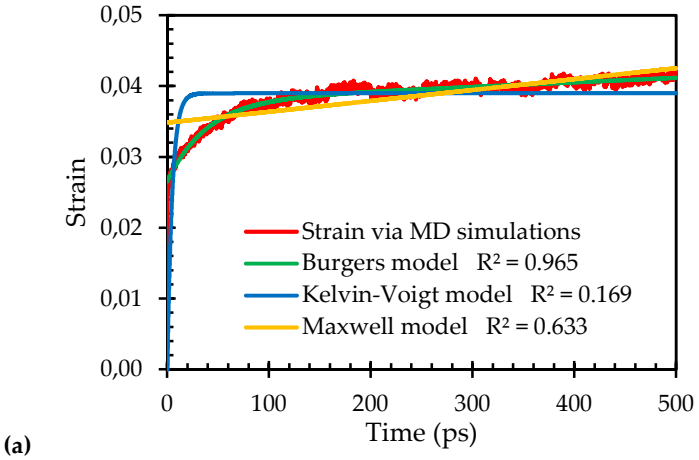

(a)

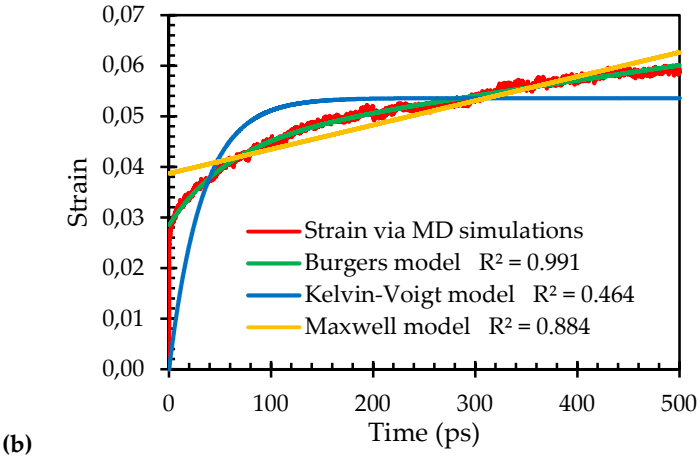

(b)

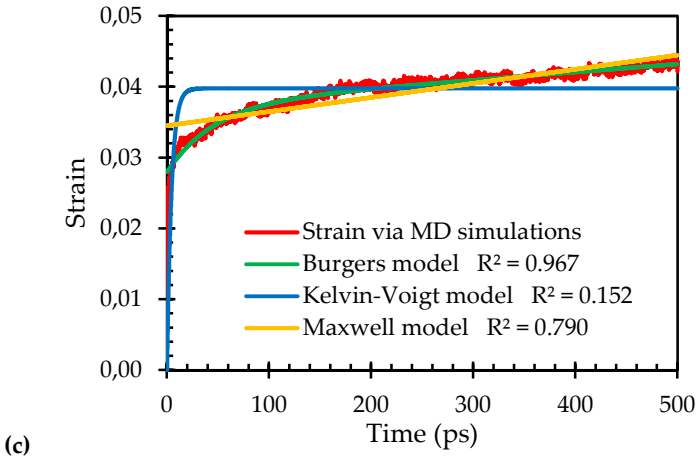

(c)

FIGURE 5. Strain versus time curves of C-S-H (I)/vacuum (1 Å)/C-S-H (I) composite in different orientations: (a) y-direction, (b) counterclockwise rotated in y-direction, and (c) z-direction.

Additionally, the 3.1 Å interfacial water layer produced higher oscillations compared to the 1 Å interfacial vacuum layer. They also exhibited lower strain values since they were under lower values of load during the creep tests.

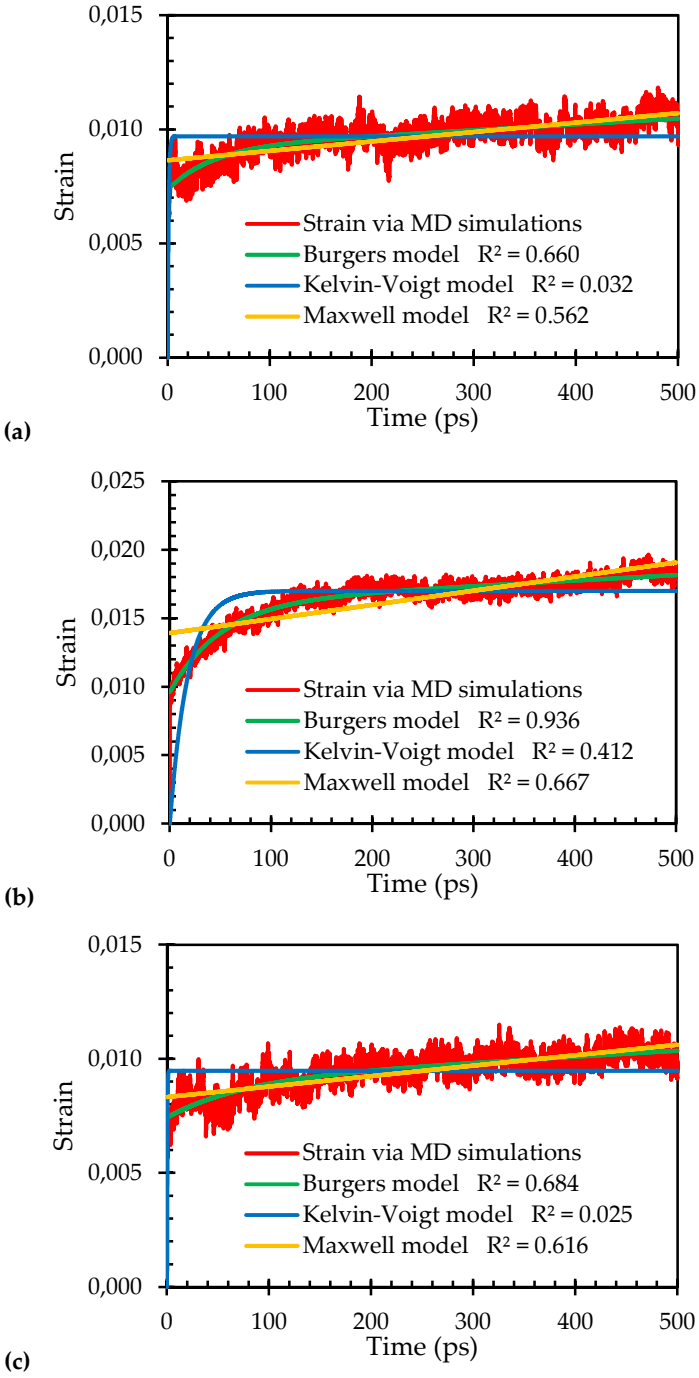

FIGURE 6. Strain versus time curves of C-S-H (I)/water (3.1 Å)/C-S-H (I) composite in different orientations: (a) y-direction, (b) counterclockwise rotated in y-direction, and (c) z-direction.

After fitting the curves using the Burgers model, Young's modulus and viscosity of Maxwell and Kelvin-Voigt sections have been obtained as shown in Table 2. These parameters might be able to used as the input parameters in the upper-scale simulations, i.e., the hardened cement paste.

TABLE 2. **Fitting parameters via Burgers model.**

Spacing	Orientation	σ_0 (GPa)	E_K (GPa)	η_K Pa.s	E_M (GPa)	η_M (Pa.s)	Running time (hr:min)
1 Å vacuum	y-direction	1.37	120.0	4.6	51.6	213.6	24:28
	counterclockwise rotated in y-direction	1.34	80.0	4.8	47.1	45.3	24:38
	z-direction	1.40	146.2	6.8	50.0	123.8	23:40
3.1 Å water	y-direction	0.34	183.1	8.0	45.9	133.6	27:10
	counterclockwise rotated in y-direction	0.43	65.7	3.3	44.7	108.6	27:38
	z-direction	0.32	192.0	14.3	42.8	124.8	26:02

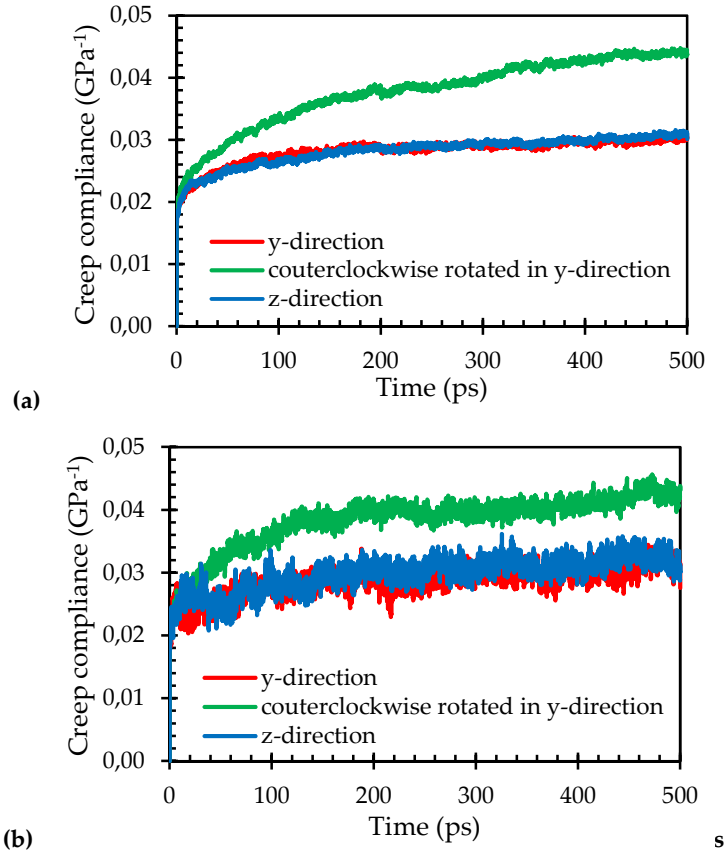

FIGURE 7. **Creep compliance curves of (a) C-S-H (I)/vacuum (1 Å)/C-S-H (I) and (b) C-S-H (I)/water (3.1 Å)/C-S-H (I) composite in different orientations.**

Creep compliance could be obtained as well as shown in Fig. 7. The creep compliances have a similar behaviour and magnitude between the C-S-H (I)/vacuum (1 Å)/C-S-H (I) and the C-S-H (I)/ water (3.1 Å)/C-S-H (I) composite in different orientations. In these curves, the influence of water seems less significant. By comparing results obtained with vacuum spacing and water spacing, the

influence of water seems not significant. Indeed, the compliance curves are similar. It means that creep of C-S-H cannot be attributed only to the adsorbed water displacement. The use of these compliance properties at the upper scale is necessary to have an idea at long term at the concrete scale.

V. CONCLUSION

To summarize, these results highlight the potential of using molecular dynamics simulations to examine the creep property of the main hydrated cement phase. In this study, the combination of hydrated cement phase was referred to as a "composite." Various spacing configurations and orientations were investigated. The orientations studied included: (a) the C-S-H (I) phase beside the C-S-H (I) phase in the y-direction, (b) the counterclockwise rotated C-S-H (I) phase around the x-axis beside the C-S-H (I) phase in the y-direction, and (c) the C-S-H (I) phase placed on top of the C-S-H (I) phase in the z-direction. The interfacial layers configurations were 1 Å vacuum layer and 3.1 Å water layer. These interfacial vacuum/water layers were placed at the interface between the relaxed C-S-H (I) composite. Creep tests were done on the C-S-H (I) composite. The results demonstrated that both the orientations and the interfacial vacuum/water layers could affect the strain versus time curves. On the other hand, Burgers model was used to fit the curves of the strain versus time. With the high values of coefficient of determination, Burgers model could represent well the strain versus time curves. These findings can serve as input parameters for higher-scale simulations, such as those at the microscopic scale of hardened cement paste. The influence of adsorbed water on the creep of C-S-H is not significant in comparison with results obtained with vacuum spacing. It encourages to analyze this behaviour under more various conditions and to propose simulation at the upper scale to see if the adsorbed water can play an important role as supposed by many authors.

REFERENCES

Bekrine, I., Hilloulin, B., Loukili, A., 2025. Investigation of the creep properties of blended cement pastes using combined nanoindentation and SEM imaging. Construction and Building Materials 463, 140103. https://doi.org/10.1016/j.conbuildmat.2025.140103

Bonnaud, P.A., Labbez, C., Miura, R., Suzuki, A., Miyamoto, N., Hatakeyama, N., Miyamoto, A., Vliet, K.J.V., 2016. Interaction grand potential between calcium–silicate–hydrate nanoparticles at the molecular level. Nanoscale 8, 4160–4172. https://doi.org/10.1039/C5NR08142D

Esposito, L., Casagrande, L., Menna, C., Asprone, D., Auricchio, F., 2021. Early-age creep behaviour of 3D printable mortars: Experimental characterisation and analytical modelling. Mater Struct 54, 207. https://doi.org/10.1617/s11527-021-01800-z

Fu, J., Bernard, F., Kamali-Bernard, S., 2018a. Assessment of the elastic properties of amorphous calcium silicates hydrates (I) and (II) structures by molecular dynamics simulation. Molecular Simulation 44, 285–299. https://doi.org/10.1080/08927022.2017.1373191

Fu, J., Kamali-Bernard, S., Bernard, F., Cornen, M., 2018b. Comparison of mechanical properties of C-S-H and portlandite between nano-indentation experiments and a modeling

approach using various simulation techniques. Composites Part B: Engineering 151, 127–138. https://doi.org/10.1016/j.compositesb.2018.05.043

Guo, M., Grondin, F., Loukili, A., 2019. Numerical method to model the creep of recycled aggregate concrete by considering the old attached mortar. Cement and Concrete Research 118, 14–24. https://doi.org/10.1016/j.cemconres.2019.01.008

Hamid, S.A., 1981. The crystal structure of the 11Å natural tobermorite Ca2.25[Si3O7.5(OH)1.5] · 1H2O. Zeitschrift für Kristallographie - Crystalline Materials 154, 189–198. https://doi.org/10.1524/zkri.1981.154.3-4.189

Hewlett, P.C., 1998. Lea's Chemistry of Concrete and Cement. Elsevier, Oxford.

Hoeun, S., Bernard, F., Grondin, F., Kamali-Bernard, S., Alam, S.Y., 2023. Elastic constants of nano-scale hydrated cement paste composites using reactive molecular dynamics simulations to homogenization of hardened cement paste mechanical properties. Materials Today Communications 106671. https://doi.org/10.1016/j.mtcomm.2023.106671

Ioannidou, K., 2020. Mesoscale Structure and Mechanics of C-S-H, in: Andreoni, W., Yip, S. (Eds.), Handbook of Materials Modeling: Applications: Current and Emerging Materials. Springer International Publishing, Cham, pp. 1–15. https://doi.org/10.1007/978-3-319-50257-1_127-1

Keinde, D., Kamali-Bernard, S., Bernard, F., Cisse, I., 2014. Effect of the interfacial transition zone and the nature of the matrix-aggregate interface on the overall elastic and inelastic behaviour of concrete under compression: a 3D numerical study. European Journal of Environmental and Civil Engineering 18, 1167–1176. https://doi.org/10.1080/19648189.2014.896757

Lau, D., Jian, W., Yu, Z., Hui, D., 2018. Nano-engineering of construction materials using molecular dynamics simulations: Prospects and challenges. Composites Part B: Engineering 143, 282–291. https://doi.org/10.1016/j.compositesb.2018.01.014

Liang, Y., 2020. Mechanical and fracture properties of calcium silicate hydrate and calcium hydroxide composite from reactive molecular dynamics simulations. Chemical Physics Letters 761, 138117. https://doi.org/10.1016/j.cplett.2020.138117

Liu, L., Jaramillo-Botero, A., Goddard, W.A., Sun, H., 2012. Development of a ReaxFF Reactive Force Field for Ettringite and Study of its Mechanical Failure Modes from Reactive Dynamics Simulations. J. Phys. Chem. A 116, 3918–3925. https://doi.org/10.1021/jp210135j

Plimpton, S., 1995. Fast Parallel Algorithms for Short-Range Molecular Dynamics. Journal of Computational Physics 117, 1–19. https://doi.org/10.1006/jcph.1995.1039

Rhardane, A., Alam, S.Y., Grondin, F., 2022. The role of surface micro-cracks in cementitious materials responsible for the Pickett effect. Mech Time-Depend Mater 26, 719–740. https://doi.org/10.1007/s11043-021-09509-w

Stukowski, A., 2009. Visualization and analysis of atomistic simulation data with OVITO–the Open Visualization Tool. Modelling Simul. Mater. Sci. Eng. 18, 015012. https://doi.org/10.1088/0965-0393/18/1/015012

van Duin, A.C.T., Dasgupta, S., Lorant, F., Goddard, W.A., 2001. ReaxFF: A Reactive Force Field for Hydrocarbons. J. Phys. Chem. A 105, 9396–9409. https://doi.org/10.1021/jp004368us